Anal. Chem. **2007,** *79,* 6933−6940

X-ray Absorption Fine Structure Combined with X-ray Fluorescence Spectroscopy. Monitoring of Vanadium Sites in Mesoporous Titania, Excited under Visible Light by Selective Detection of Vanadium K$\beta_{5,2}$ Fluorescence

Yasuo Izumi,*,† Kazushi Konishi,‡ Diaa Mosbah Obaid,‡ Tomohisa Miyajima,§ and Hideaki Yoshitake§

Department of Chemistry, Graduate School of Science, Chiba University, Yayoi 1-33, Inage-ku, Chiba 263-8522, Japan, Interdisciplinary Graduate School of Science and Engineering, Tokyo Institute of Technology, Nagatsuta 4259, Midori-ku, Yokohama 226-8502, Japan, and Graduate School of Engineering, Yokohama National University, Tokiwadai 79-5, Hodogaya-ku, Yokohama 240-8501, Japan

The photocatalytic role of vanadium doped in mesoporous TiO_2 has not been clarified. Valence state-sensitive V K$\beta_{5,2}$-selecting (5462.9 eV) X-ray absorption fine structure (XAFS) was used to monitor the V sites in mesoporous TiO_2 for ethanol dehydration under equilibrium in situ conditions and visible light-illumination. First, the feasibility of discriminating V^{IV} sites from a 1:1 physical mixture of standard V^{IV} and V^{V} inorganic compounds was demonstrated, by tuning the secondary fluorescence spectrometer to 5459.0 eV. The chemical shift of V K$\beta_{5,2}$ emission between V^{IV} and V^{V} sites was 1.0 eV. The selection of valence states V^{IV} and V^{V} was 100% and 80%, respectively. The redox states for ethanol dehydration over mesoporous TiO_2 excited in visible light were suggested to be V^{III} and V^{IV}. The chemical shift between valence states V^{III} and V^{IV} was greater (3.2 eV). On the basis of V K$\beta_{5,2}$ emission and V K$\beta_{5,2}$-selecting XAFS spectra tuned to the V K$\beta_{5,2}$ peak, we determined that the fresh mesoporous V−TiO_2 catalyst has a valence state of V^{IV}. The vanadium sites were partially reduced by the dissociative adsorption of ethanol under visible light, but they still stay within the emission-energy ranges for standard V^{IV} compounds. These partially reduced vanadium sites were reoxidized in oxygen under visible light. Finally, direct XAFS observation of photoreduced V^{III} sites was attempted by tuning the fluorescence spectrometer to 5456.3 eV for partially reduced mesoporous V−TiO_2. Valence state V^{III} was selected for 60% of the spectrum in the mixture of V^{III} (minor) and V^{IV} (dominant) valence states.

Solar energy provides clean energy. One possibility for solar technology is photocatalysis over TiO_2-based catalysts. Only 3% of solar energy is used by anatase-type TiO_2 at the surface of the earth. However, this efficiency can be improved by doping with V, Cr, Mn, Fe, Ni,[1] C, N, or S atoms.[2,3] Under visible light illumination, V doping on/in TiO_2 improves oxidation of ethanol[4] and degradation of crystal violet, methylene blue,[5,6] methyl orange,[7] and nitric oxide.[8]

We recently reported V doping effects in mesoporous TiO_2 with a specific surface area (SA) as large as 1200 $m^2\ g^{-1}$.[9] Under visible light, mesoporous TiO_2 exhibited poor activity (Table 1, entry b). After doping with 1−3 wt % of V, the catalyst proceeded with the dehydration of ethanol (1.0 kPa) to produce acetaldehyde and water (Table 1, entry c), in clear contrast to the ethanol dehydrogenation over [V-doped] mainly anatase-type TiO_2 catalysts (Table 1, entry a). Because the V addition sometimes hampers photocatalysis of TiO_2,[10] it is critical to understand the catalytic role of V under visible light. The promoting role of V is still unclear for the mesoporous V−TiO_2 catalysts.[9]

Monitoring low concentrations of V on/in the TiO_2 matrix using XAFS is technically difficult, because the V K-edge absorption energy is in the extended X-ray absorption fine structure (EXAFS) region for high Ti concentrations. Selective detection of V Kα_1 fluorescence (4952.2 eV) from Ti K$\beta_{1,3}$ (4931.8 eV) emitted from a sample is impossible using conventional pulse-type X-ray detectors with energy resolutions greater than 35%.[11] V Kα_1-selecting XAFS with a high energy-resolution fluorescence

* Corresponding author. E-mail: yizumi@faculty.chiba-u.jp.
† Chiba University.
‡ Tokyo Institute of Technology.
§ Yokohama National University.

(1) Anpo, M. *Bull. Chem. Soc. Jpn.* **2004**, *77* (8), 1427−1442.
(2) Khan, S. U. M.; Al-Shahry, M.; Ingler, W. B., Jr. *Science* **2002**, *297*, 2243−2245.
(3) Aita, Y.; Komatsu, M.; Yin, S.; Sato, T. *J. Solid State Chem.* **2004**, *177* (9), 3235−3238.
(4) Klosek, S.; Raftery, D. *J. Phys. Chem. B* **2001**, *105* (14), 2815−2819.
(5) Iketani, K.; Sun, R. D.; Toki, M.; Hirota, K.; Yamaguchi, O. *Mater. Sci. Eng., B* **2004**, *108*, 187−193.
(6) Wu, J. C. S.; Chen, C. H. *J. Photochem. Photobiol., A* **2004**, *163*, 509−515.
(7) Hou, X. G.; Hao, F. H.; Fan, B.; Gu, X. N.; Wu, X. Y.; Liu, A. D. *Nucl. Instrum. Methods Phys. Res., Sect. B* **2006**, *243*, 99−102.
(8) Yamashita, H.; Ichihashi, Y.; Takeuchi, M.; Kishiguchi, S.; Anpo, M. *J. Synchrotron Radiat.* **1999**, *6*, 451−452.
(9) Masih, D.; Yoshitake, H.; Izumi, Y. *Appl. Catal., A* **2007**, *325* (2), 276−282.
(10) Martin, S. T.; Morrison, C. L.; Hoffmann, M. R. *J. Phys. Chem.* **1994**, *98* (51), 13695−13704.

10.1021/ac070427p CCC: $37.00
Published on Web 08/22/2007

Table 1. Products Formation Rates in the Ethanol Photo-Oxidation (55 μmol of Ethanol, 110 μmol of O_2) over [V]−TiO_2 Catalysts under Visible Light (>420 nm)[9]

		formation rates (μmol h^{-1} g_{cat}^{-1})		
entry	catalyst	CH_3CHO	H_2O	CO_2
a	TiO_2 (P-25)[b]	19	4.9	0.2
b	mesoporous TiO_2	2.3	16	0.3
c	mesoporous V−TiO_2[c]	23	212 (16[a])	0.3

[a] Steady-state rate later than 1 h of reaction. [b] Anatase/rutile = $^3/_1$. [c] 3.0 wt % V.

Scheme 1. Energy Diagram of V K$\beta_{5,2}$ and V Kα_1 Emission Processes and of Catalysis over Mesoporous V−TiO_2 under the Illumination of Visible Light

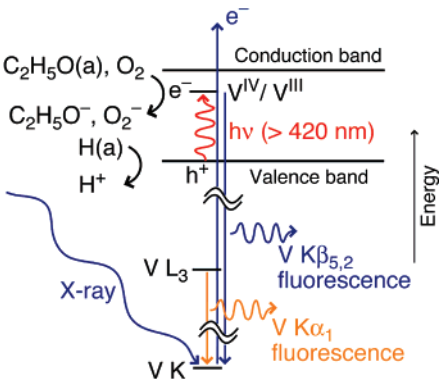

spectrometer was used to selectively monitor the 0.6−10.4 wt % of V sites on/in TiO_2.[12−14] This wavelength-dispersive spectrometer is compared with energy-dispersive detectors, e.g., a Ge solid-state detector, Si drift detector, or PIN-diode detector. The energy resolution of these latter detectors is 2−3%, not enough to discriminate between V Kα_1 and Ti K$\beta_{1,3}$. They also are limited by a maximum count rate under the large background of Ti K fluorescence.[15]

In this study, to monitor the V sites in mesoporous TiO_2 under visible light, V K$\beta_{5,2}$ fluorescence (5462.9 eV)[16] associated with the electronic transition from the frontier valence electronic level(s) to the K level was selected. The valence level is closely related to the electron−hole pair formation at the band gap excited under visible light (Scheme 1). Scheme 1 also depicts the energy diagram for V K$\beta_{5,2}$ emission, comparing it with that for V Kα_1 emission. A major advantage of V K$\beta_{5,2}$-selecting XAFS is better site discrimination because of greater chemical shifts of V K$\beta_{5,2}$ emission compared with V Kα_1-selecting XAFS. The mesoporous V−TiO_2 catalysts were set under *on-reaction* conditions (in

(11) Heald, S. M. In *X-Ray Absorption: Principles, Applications, Techniques of EXAFS, SEXAFS, and XANES*; Koningsberger, D. C., Prins, R., Eds.; John Wiley & Sons: New York, 1988; pp 87−118.
(12) Izumi, Y.; Kiyotaki, F.; Yagi, N.; Vlaicu, A. M., Nisawa, A.; Fukushima, S.; Yoshitake, H.; Iwasawa, Y. *J. Phys. Chem. B* **2005**, *109* (31), 14884−14891.
(13) Izumi, Y.; Kiyotaki, F.; Yoshitake, H.; Aika, K.; Sugihara, T.; Tatsumi, T.; Tanizawa, Y.; Shido, T.; Iwasawa, Y. *Chem. Lett.* **2002**, 1154−1155.
(14) Izumi, Y.; Kiyotaki, F.; Yoshitake, H.; Aika, K.; Sugihara, T.; Tatsumi, T.; Tanizawa, Y.; Shido, T.; Iwasawa, Y. *Chem. Commun.* **2002**, 2402−2403.
(15) Izumi, Y.; Kiyotaki, F.; Minato, T.; Seida, Y. *Anal. Chem.* **2002**, *74* (15), 3819−3823.
(16) (a) Bearden, J. A. *Rev. Mod. Phys.* **1967**, *39*, 78−124. (b) Zschornack, G. *Handbook of X-Ray Data*; Springer: Berlin/Heidelberg, 2007.

Scheme 2. Schematic View of the Fluorescence Spectrometer Combined with the XAFS Beamline for V K$\beta_{5,2}$-Selecting XAFS Measurements under the Illumination of Visible Light

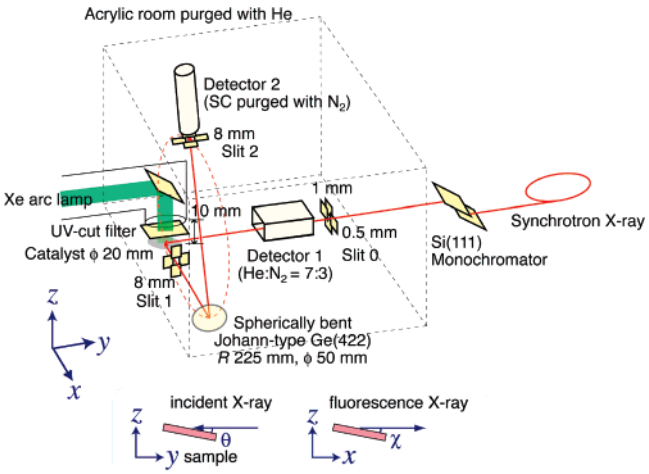

substrate under visible light) during the V K$\beta_{5,2}$-selecting V K-edge XAFS measurements.

METHODS

Samples. Vanadium metal (25 μm thickness, 99.7%; Aldrich), V_2O_3 (99.99%, Aldrich), $VO(SO_4)\cdot nH_2O$ (99.9%, Wako), and Na_3VO_4 (Wako) were used as received. The powders and the physical mixture of $V^{IV}O(SO_4)\cdot nH_2O$ and $Na_3V^{V}O_4$ (1:1 on the basis of the V amount) were thoroughly mixed with boron nitride (Wako) to 3 wt % V and pressed into a 20 mm-diameter disk.

The preparation of mesoporous V−TiO_2 catalysts was followed from literature.[17] In brief, an aqueous solution of vanadium triisopropoxide oxide, titanium tetraisopropoxide, and dodecylamine was maintained at 333 K for 6 days and then filtered. The resulting powder was maintained at 453 K for 10 days, and then washed with *p*-toluenesulfonic acid in ethanol. The V content was fixed to 3.0 wt % in this study, corresponding to a V/Ti atomic ratio of 1/21.

X-ray Measurements. The X-ray measurements were performed in the Photon Factory at the High-Energy Accelerator Research Organization (KEK-PF, Tsukuba), on the bending-magnet beamline 9C for standard V compounds and on the bending-magnet beamline 7C for the V catalysts at 290 K. The storage-ring energy was 2.5 GeV and the ring current was between 449 and 281 mA. A Si(111) double crystal monochromator and a focusing/higher-harmonics-rejection mirror were inserted. The X-ray beam was focused at the sample position and fully tuned.

The sample's X-ray fluorescence was analyzed with a home-made fluorescence spectrometer (Scheme 2) as described in the literature.[18] The dimensions of the slit openings were as follows. Slit 0: 0.5 (horizontal) × 1.0 (vertical) mm. Slit 1 and slit 2: 8.0 (horizontal) × 8.0 (vertical) mm. The sample was set on a plane near the horizontal plane, and the sample surface was tilted from the horizontal plane toward the incident X-ray beam by 6.0° and

(17) Yoshitake, H.; Tatsumi, T. *Chem. Mater.* **2003**, *15* (8), 1695−1702.
(18) Izumi, Y.; Nagamori, H.; Kiyotaki, F.; Masih, D.; Minato, T.; Roisin, E.; Candy, J. P.; Tanida, H.; Uruga, T. *Anal. Chem.* **2005**, *77* (21), 6969−6975.

toward the Ge analyzer crystal by 7.0° (see Scheme 2, bottom). Detectors 1 and 2 were an ionization chamber (S1194−B1, Oken) purged with a mixture of helium and nitrogen (7:3) and a NaI(Tl) scintillation counter (SP10, Oken), respectively. The sample, detector 2, and a spherically bent Johann-type Ge(422) 50-mm-diameter crystal (d = 1.1547 Å) (Saint Gobain) were set in the Rowland configuration. The crystal's curvature radius was 450 mm. The spectrometer was purged with helium. Detector 2 was purged with nitrogen gas to avoid discharging the preamplifier. The sample section was covered with a 1 mm thick lead plate housing, except for the openings for the incident X-ray beam and the exit of X-ray fluorescence from the sample.

The sample disk of mesoporous V−TiO_2 was set in an *on-reaction* cell equipped with a 16 μm thick polyethylene naphthalate window (Q51-16, Teijin). The sample was positioned 10 mm from the exit window of the Xe arc lamp (500 W, UXL-500D, Ushio). A UV-cut filter L42 (cutoff wavelength 420 nm, Kenko) was set between them (Scheme 2). The fresh sample was in argon, and 2.1 kPa of ethanol was introduced followed by illumination by visible light for 7 h. Under these conditions, the conversion rate from ethanol to acetaldehyde was 12% h^{-1}. After the arc lamp was turned off, 101 kPa of oxygen was introduced for 2 h, followed by visible light illumination for 7 h.

The V K$\beta_{5,2}$ emission spectra were measured for standard inorganic V compounds and mesoporous V−TiO_2 catalysts by scanning the fluorescence spectrometer with the excitation energy fixed at 5484.1 eV. The emission energy for the V metal was calibrated to 5462.9 eV (Bragg angle θ_B = 79.335°).[16] The scan step of the emission energy was ≈0.36 eV and the accumulation time was 60−90 s per point. The count rates of emitted photons measured by detector 2 were 10^2−10^1 and 15−5 counts s^{-1} for standard V compounds and V−TiO_2 catalysts, respectively.

The V K$\beta_{5,2}$-selecting V K-edge XAFS spectrum was measured by tuning the fluorescence spectrometer to fixed emission energies around the V K$\beta_{5,2}$ emission peak. The scan step of photon energy was ≈0.25 eV and the accumulation time was 60−100 s per point. The data obtained were smoothed with a weighted curve-fit program with 3% smoothing factor in pre-edge and 10% in post-edge regions, respectively. The original and smoothed data were carefully compared to prevent changing the energy and shape of all peaks and absorption edges. The V K-edge energy for V metal was calibrated to 5463.9 eV.[16] The energy positions of the monochromator and the fluorescence spectrometer were reproduced within ±0.1 and ±0.2 eV, respectively. Energy resolution of the fluorescence spectrometer was evaluated to be 1.1 eV at the energy of V K$\beta_{5,2}$.[12]

Analysis. The XAFS data analysis was performed with the software package XDAP version 2.2.7 (XAFS Services International) based on the works of M. Vaarkamp, H. Linders, and D. Koningsberger. The analysis procedure was already described in ref 12. In brief, the pre-edge background was approximated by the modified Victoreen function $C_2/E^2 + C_1/E + C_0$. The background of post-edge oscillations was approximated by a smoothing-spline function, calculated by the equation for the number of data points N.

$$\sum_{i=1}^{N} \frac{(\mu x_i - BG_i)^2}{\exp(-0.075k_i^2)} \leq \text{smoothing factor}$$

The similarity of the XANES spectra (spectral fit) was evaluated based on the R-factor.

$$R_f = \frac{\int |\chi^{\text{observed data}}(k) - \chi^{\text{reference data}}(k)|^2 \, dk}{\int |\chi^{\text{observed data}}(k)|^2 \, dk}$$

RESULTS

V K$\beta_{5,2}$ Emission Spectra. The V K$\beta_{5,2}$ emission spectra measured for V^0 metal, $V^{III}_2O_3$, $V^{IV}O(SO_4)\cdot nH_2O$, and $Na_3V^VO_4$ are shown in Figure 1A. Intense peaks appeared, centered at 5462.9 (a), 5458.7 (b), 5461.9 (c), and 5462.9 eV (d), respectively, accompanied by a weaker shoulder on the lower-energy side, between 5457 and 5461 eV, except for in V_2O_3. The lower-energy side shoulder is not observed for V_2O_3 because the fluorescence spectrometer (θ_B < 79.94°) cannot measure spectra lower than 5452.5 eV (Kβ'' peak region ≈ 5448 eV).[19−21] The relative intensity of the shoulder was the highest for $V^{IV}O(SO_4)\cdot nH_2O$ (Figure 1A, spectrum c). The effect of the V K$\beta_{1,3}$ (5427.3 eV)[16] tail was negligible within the energy resolution of the fluorescence spectrometer, 1.1 eV in this study. Assuming a V K$\beta_{5,2}$/V K$\beta_{1,3}$ peak-intensity ratio of $^1/_{30}$ to $^1/_{10}$[20] and a pseudo-Voigt type peak shape, the tail contribution of V K$\beta_{1,3}$ was estimated at only 1.8−0.6% of the V K$\beta_{5,2}$ peak intensity at 5462.9 eV.

These peak energy values were consistent with reported values: 5458.8−5460.5, 5460.5−5462.3, and 5462.5−5464.2 eV for standard V^{III}, V^{IV}, and V^V compounds, respectively (Table 2).[19−21] The minor discrepancy for V_2O_3 may result from the difference between energy resolution of the fluorescence spectrometer used in this work and the ones used in the references. In particular, because the K$\beta_{5,2}$ main peak was accompanied by a shoulder peak, the main peak's maximum energy may vary, depending on peak width, because of energy-resolution differences. The V K$\beta_{5,2}$ emission spectrum of the 1:1 physical mixture of $V^{IV}O(SO_4)\cdot nH_2O$ and $Na_3V^VO_4$ was compared with spectra of $VO(SO_4)\cdot nH_2O$ (Figure 1A, spectrum c) and Na_3VO_4 (Figure 1A, spectrum d). The former spectrum was well reproduced by the weighted sum of the spectrum for each compound with a mixing ratio of 1:1.

The V K$\beta_{5,2}$ emission spectra measured for mesoporous V−TiO_2 are shown in Figure 1B. The intense peak for the fresh sample at 5462.1 eV (spectrum a) shifted progressively toward the lower-energy side to 5461.6 eV in ethanol (spectrum b), then to 5461.0 eV in ethanol under visible light (spectrum c). After the visible light was turned off, the peak moved up to 5461.6 eV (spectrum d). The sample was then exposed to oxygen and illuminated by visible light (spectrum e). The peak increased to 5462.4 eV (Table 2). The shoulder on the lower-energy side constantly appeared in spectra a−e, but its intensity was greatest in spectrum d (5456.3 eV). The different background at lower energy shown in Figure 1B may be an experimental artifact. The

(19) Jones, J. B.; Urch, D. S. *J. Chem. Soc., Dalton Trans.* **1975**, 1885−1889.
(20) Yasuda, S.; Kakiyama, K. *X-Ray Spectrom.* **1978**, *7* (1), 23−25.
(21) Werfel, F.; Dräger, G.; Berg, U. *Cryst. Res. Technol.* **1981**, *16* (1), 119−126.

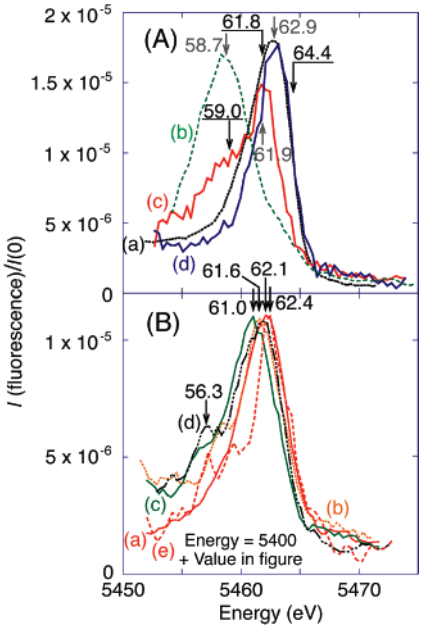

Figure 1. V K$\beta_{5,2}$ emission spectra (A) for (a) V metal, (b) V_2O_3, (c) $VO(SO_4)\cdot nH_2O$, and (d) Na_3VO_4 and (B) mesoporous V−TiO_2 catalyst as (a) fresh in argon, (b) in 2.1 kPa of ethanol, (c) in ethanol under the illumination of visible light, (d) after the visible light was turned off, and (e) in 101 kPa of O_2 under visible light (e). The excitation energy was fixed at 5484.1 eV. The peak intensity reduced to $^1/_{20}$ and $^1/_4$ for spectra a in part A and spectra b in part A, respectively. The arrows indicate the tuned energy for selective V K-edge measurements in Figures 2 and 3.

amount of remaining gases, other than helium, may have decreased as the helium purge continued inside the fluorescence spectrometer during the data scan.

Discrimination between V^{IV} and V^V Sites in V K-Edge XANES for Mixed Standard Compounds. With the use of the physical mixture of $V^{IV}O(SO_4)\cdot nH_2O$ and $Na_3V^VO_4$, the fluorescence spectrometer was tuned to 5459.0, 5461.8, or 5464.4 eV to check the feasibility of V^{IV} and V^V site discrimination using the V K$\beta_{5,2}$-selecting XAFS. The energies of 5459.0 and 5464.4 eV corresponded to the lower-energy shoulder of V^{IV} emission (the smaller contribution of V^V at the foot of V^V emission) and the half-intensity energy of V^V emission on the higher-energy side (the smaller contribution of V^{IV} at the foot of V^{IV} emission), respectively. Each tuned energy is depicted as an arrow in Figure 1A.

The XANES (X-ray absorption near-edge structure) spectrum obtained by tuning to 5459.0 eV (Figure 2B, spectrum a) resembled that for $V^{IV}O(SO_4)\cdot nH_2O$ (Figure 2A. spectrum b) (R_f = 0.20%; Figure 2B, inset of spectrum a and Figure S1 spectrum a in the Supporting Information). This demonstrated the feasibility of discriminating V^{IV} sites from V^V sites. However, the intensity of the pre-edge peak at 5468.3 eV (Figure 2B, spectrum a) was 2.1 times greater than in Figure 2A, spectrum b. This pre-edge peak may be enhanced because of resonance-excitation effects, similar to that seen in reports for Fe K$\beta_{1,3}$-selecting,[22] Cu Kα_1-selecting,[18] and Sn Kα_1-selecting XANES.[18] Typically, discrepancies between V K$\beta_{5,2}$-selecting XANES spectra and those measured in the transmission mode[17] occurred in the pre-edge peak region. The relatively broad spectral features above 5473 or 5474 eV are relatively similar within the energy resolution of the fluorescence spectrometer used in this work (1.1 eV).

As the tuned energy of the fluorescence spectrometer increased to 5461.8, and then to 5464.4 eV, the absorption-edge position of the XANES spectra shifted to 5480.6 (Figure 2B, spectrum b) and then to 5481.3 eV (Figure 2B, spectrum c). The spectrum c in Figure 2B was the most similar to the weighted sum of two spectra for $V^{IV}O(SO_4)\cdot nH_2O$ (Figure 2A, spectrum b) and $Na_3V^VO_4$ (Figure 2A, spectrum c) with the mixing ratio of 2:8 (R_f = 0.51%; Figure 2B, inset of spectrum c and Figure S1, spectrum c). The discrimination of V^V sites from V^{IV} sites was relatively difficult because of the relatively small chemical shift between V^{IV} and V^V (1.0 eV) in the emission spectra, and the tail of the V^{IV} peak overlapped the V^V peak (Figure 1A, spectra c and d).

The site discrimination among V^{III} and V^0 or among V^{III} and V^{IV} should be easier because of their greater chemical shifts in emission spectra (3.2−4.2 eV). These feasibility tests show that V^{III} and V^V site discrimination will be possible for the mixture of V^{III}, V^{IV}, and V^V (e.g., complex heterogeneous V catalysts, but only V^{III} and V^{IV} are present for mesoporous V−TiO_2 (the catalyst in this study)). The middle V^{IV} (Figure 1A, spectrum c) will be difficult to extract. V K$\beta_{5,2}$-selecting XAFS was advantageous because of its greater chemical shifts, compared with V Kα_1-selecting XAFS (Kα_1 emission shift ≈ 0.5 eV).[12]

The pre-edge peak intensity at 5469.4 eV for XANES tuned to 5464.4 eV (Figure 2B, spectrum c) was as small as 0.23. Tsutsumi et al. reported Ti K$\beta_{5,2}$ spectra systematically for TiO_x (x = 0.4−2) and concluded that the most intense peak rose from O 2p, based on density of states calculations.[23] The tuned energy 5464.4 eV may correspond to the higher-energy side of V^V Kβ_2, derived from the electronic transition from V or oxo np to V 1s.[19,23,24] This significant suppression of pre-edge peak intensity was in contrast to the enhancement in V^{IV} K$\beta_{5,2}$-selecting XANES tuned to 5459.0 eV (Figure 2B, spectrum a).

V K$\beta_{5,2}$-Selecting XANES for Mesoporous V−TiO_2, Tuned to K$\beta_{5,2}$ Peak. V K$\beta_{5,2}$-selecting XANES spectra were measured for a mesoporous V−TiO_2 catalyst. The tuned energy was first fixed to the peaks (arrows in Figure 1B) to observe site changes systematically under each catalytic condition. With the energy resolution of the fluorescence spectrometer (1.1 eV), the predominant valence state was selected by tuning to each peak under each catalytic condition.

For the fresh sample, the pre-edge peak and rising-edge energy values were 5468.2 and 5479.7 eV, respectively (Figure 3a). These were within the ranges of corresponding values, 5467.7−5469.4 and 5476.9−5479.8 eV, respectively (Table 2), for V^{IV} standard compounds (Figure 2A, spectrum b), mesoporous V−TiO_2 (V Kα_1-selecting XANES), and mesoporous TiO_2 (Ti K-edge XANES shifted by +499.8 eV).[12] In combination with the V K$\beta_{5,2}$ emission data (see previous section), it was demonstrated that V^{IV} sites substituted on the Ti sites of the amorphous TiO_2 matrix for the incipient catalyst (Figure 4a). A major reason to suggest the V local structure in Figure 4a is that the V K-edge XANES spectral

(22) Heijboer, W. M.; Glatzel, P.; Sawant, K. R.; Lobo, R. F.; Bergmann, U.; Barrea, R. A.; Koningsberger, D. C.; Weckhuysen, B. M.; de Groot, F. M. F. *J. Phys. Chem. B* **2004**, *108*, 10002−10011.

(23) Tsutsumi, K.; Aita, O.; Ichikawa, K. *Phys. Rev. B* **1977**, *15* (10), 4638−4643.

(24) Glatzel, P.; Bergmann, U. *Coord. Chem. Rev.* **2005**, *249*, 65−95.

Table 2. Bonding Information and Energy Values for Vanadium K$\beta_{5,2}$ Emission Peaks and Pre-Edge and Vanadium K Absorption Edges for Standard V Inorganic Compounds and the Mesoporous V−TiO_2 Catalyst

compound/condition	formal valence	bond type	no. of bonds	energy (eV)			refs
				K$\beta_{5,2}$ emission	pre-edge peak	V K absorption[g]	
V metal	0	V−V	12	5462.9		5463.9	this work
V_2O_3	3	V−O	6	5458.7	5470.2	5474.7	this work
				5459.7		5473.6	20, 28
				5458.8			21
$V(PD)_3$[a]	3	V−O	6	5460.5			19
VF_3	3	V−F	6	5459.9			19
VCl_3	3	V−Cl	6	5459.0			20
VN	3	V−N	6		5467.7	5471.6	28
VP	3	V−P	6		5467.7	5469.9	28
$VO(SO_4)\cdot nH_2O$	4	V−O	5	5461.9	5468.5	5479.4	this work
				5462.3	5468.8	5479.8	20, 12
				5460.5	5467.7	5478.5	19, 28
V_2O_4	4	V−O	6	5461.6	5469.4	5477.5	20, 12
				5462.0	5468.3	5476.9	19, 28
				5461.0			21
Na_3VO_4	5	V−O	4	5462.9	5468.7	5482.1	this work
				5464.2			20
NH_4VO_3	5	V−O	4	5463.5	5468.6	5481.3	20, 12
				5462.9	5467.7	5480.1	19, 28
V_2O_5	5	V−O	5	5463.5	5469.5	5480.0	20, 12
				5462.9	5468.5	5478.0	19, 28
				5462.5			21
mesoporous V−TiO_2	incipient (fresh)			5462.1	5468.2	5479.7	this work[b]
					5467.9	5479.8	12[c]
					5468.2	5479.7	12[d]
	in ethanol			5461.6	5468.0	5478.0[e]	this work[b]
	in ethanol, under visible light			5461.0	5468.4	5477.8	this work[b]
	in ethanol, light off			5461.6	5468.0	5479.0	this work[b]
	in O_2				5468.7	5479.8	this work[b]
	in O_2, under visible light			5462.4	5468.7	5479.9	this work[b]
mesoporous TiO_2					4968.1[f]	4978.4[f]	12

[a] PD = pentane-2,4-dionate. [b] 3.0 wt % of V. [c] 0.6 wt % of V. [d] 10.4 wt % of V. [e] Average value. [f] Titanium K-edge. [g] First derivative maximum.

pattern for mesoporous V−TiO_2 was similar to that of the Ti K-edge for mesoporous TiO_2 in terms of pre-edge and absorption-edge energy and post-edge peaks position and relative intensity.[25] This structure was supported by the curve-fit analyses for V K-edge EXAFS [N(V−O) = 4−5].[12,17] Five-coordination of Ti sites was reported for mesoporous TiO_2.[25] V^{IV} (or V^{III}) site substitution on the Ti sites of the TiO_2 matrix has been already reported.[4,6,8,12,13,26,27]

With the introduction of ethanol, the rising edge shifted toward lower energy to 5478.0 eV (average) (Figure 3b). Some vanadium sites were reduced from their native valence state (IV) because of the dissociative adsorption of ethanol on V^{IV} sites (Figure 4b). Pre-edge and post-edge peak positions and patterns were similar to those for the fresh sample (Figure 3a). Dissociative adsorption of 2-propanol was reported over mesoporous V−TiO_2 at 290 K.[12]

Next, visible light was introduced. The rising edge shifted further toward lower energy to 5477.8 eV (Figure 3c). The rising-edge positions were observed at 5469.9−5474.7, 5476.9−5479.8, and 5478.0−5482.1 eV for V^{III}, V^{IV}, and V^{V} standard inorganic compounds, respectively (Table 2).[12,28] The total edge-position shift was −1.9 eV compared with the native state; however, 5477.8 eV is still within the energy range for valence state V^{IV}.

When the visible light was turned off, the edge position oxidized back to 5479.0 eV and the pre-edge peak intensity at 5468.0 eV became fairly weak (0.21) (Figure 3d). With the introduction of atmospheric pressure oxygen under visible light, the absorption edge shifted up to 5479.9 eV (Figure 3e,f). Partially reduced V sites because of the dissociative adsorption of ethanol and visible light illumination completely oxidized back to valence state V^{IV} in oxygen and/or visible light.

Exclusive determination of the valence state is sometimes difficult because the chemical shift due to the changes of interatomic distances and coordination symmetry is plausible both in V K$\beta_{5,2}$ emission and V K$\beta_{5,2}$-selecting XANES. The change of valence state in Figure 4 was supported by a reversible trend of V K$\beta_{5,2}$ emission and V K$\beta_{5,2}$-selecting XANES and a systematic site symmetry decrease as the V content increases in mesoporous V−TiO_2.[12] In summary, V K$\beta_{5,2}$-selecting XANES spectra under each catalytic condition (parts a, b, c, and f of Figure 3) were assigned to catalytic reaction states of parts a , b, b + c, and a of Figure 4, respectively.

(25) Yoshitake, H.; Sugihara, T.; Tatsumi, T. *Chem. Mater.* **2002**, *14* (3), 1023−1029.
(26) Yu, J. C.; Lin, J.; Kwok, R. W. M. *J. Photochem. Photobiol., A* **1997**, *111*, 199−203.
(27) Kang, M.; Choi, D. H.; Choung, S. J. *J. Ind. Eng. Chem.* **2005**, *11* (2), 240−247.
(28) Wong, J.; Lytle, F. W.; Messmer, R. P.; Maylotte, D. H. *Phys. Rev. B* **1984**, *30* (10), 5596−5610.

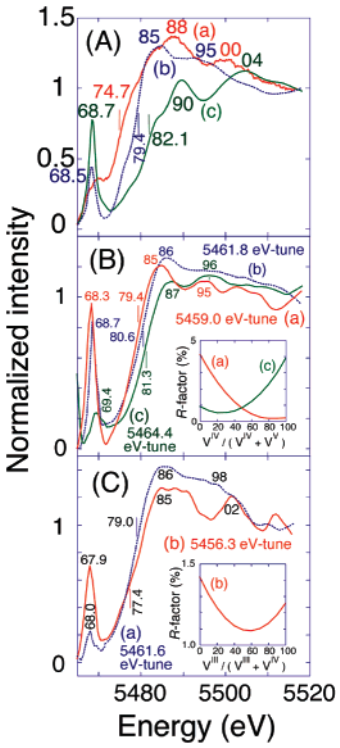

Figure 2. (A) V K-edge XANES spectra for (a) V_2O_3, (b) $VO(SO_4)\cdot nH_2O$, and (c) Na_3VO_4 measured in the transmission mode. (B) V K$\beta_{5,2}$-detecting V K-edge XANES spectra for the 1:1 physical mixture of $V^{IV}O(SO_4)\cdot nH_2O$ and $Na_3V^{V}O_4$. The tuned energy was (a) 5459.0, (b) 5461.8, and (c) 5464.4 eV. Inset: *R*-factor change-of-fit for spectra a and c with those for $VO(SO_4)\cdot nH_2O$ and Na_3VO_4 by changing the mixing ratio. The fits were performed in energy ranges above 5474 eV. (C) V K$\beta_{5,2}$-detecting V K-edge XANES spectra for the mesoporous V−TiO_2 catalyst after visible-light illumination in 2.1 kPa of ethanol. The tuned energy was (a) 5461.6 and (b) 5456.3 eV. Inset: *R*-factor change-of-fit for spectrum b with those for V_2O_3 and $VO(SO_4)\cdot nH_2O$. The fits were performed in energy ranges above 5473 eV.

V K$\beta_{5,2}$-Selecting XANES for Mesoporous V−TiO_2, Tuned to the Shoulder of K$\beta_{5,2}$. For the partially reduced mesoporous V−TiO_2 sample for Figure 1B, spectra d and Figure 3d, the fluorescence spectrometer was tuned to 5456.3 eV (arrow in Figure 1B) to specifically discriminate V^{III} and compare with XANES spectrum tuned to the top of the V K$\beta_{5,2}$ peak. Figure 2C, spectrum b shows the obtained V K-edge XANES spectrum compared with spectrum a, tuned to 5461.6 eV. The rising-edge position at 5477.4 eV is shifted by −1.6 eV, compared with spectrum a. The energy was within the range for standard V^{IV} compounds (Table 2).

The spectral pattern above 5473 eV was most similar to the weighted sum of standard spectra for V^{III} and V^{IV} with a mixing ratio 6:4 (Figure 2A, spectra a, b) (R_f = 1.1%; Figure 2C, inset). The V sites for the two model compounds are surrounded by five to six O atoms (Table 2) similar to the V-site coordination for mesoporous V−TiO_2.[12,17] Thus, this trial did not detect a fully reduced valence state (V^{III}) by excited electrons under visible light. Because the V^{III} site selection (60%) was evaluated using the XANES spectrum for standard $V^{III}_2O_3$, data subtraction of XANES for the valence state V^{IV} (40%, Figure 3a) to computationally extract the valence state V^{III} in the catalyst may lead to uncertainty,

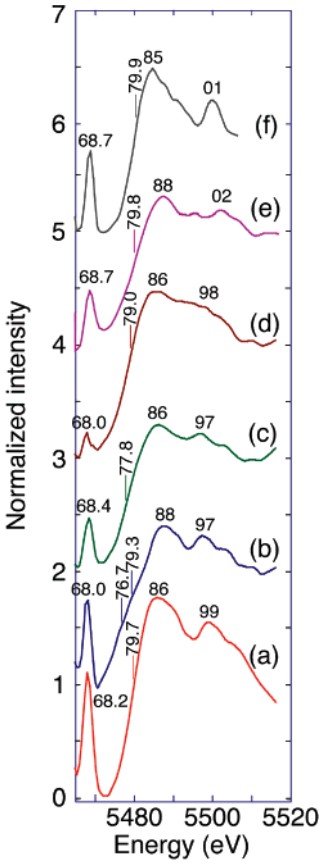

Figure 3. V K$\beta_{5,2}$-detecting V K-edge XANES spectra for the mesoporous V−TiO_2 catalyst. (a) Fresh sample in argon, (b) in 2.1 kPa of ethanol, (c) in ethanol under visible light, (d) after the visible light was turned off, (e) in 101 kPa of O_2, and (f) in O_2 under visible light. The tuned energies were 5462.1, 5461.6, 5461.0, 5461.6, 5462.4, and 5462.4 eV, respectively.

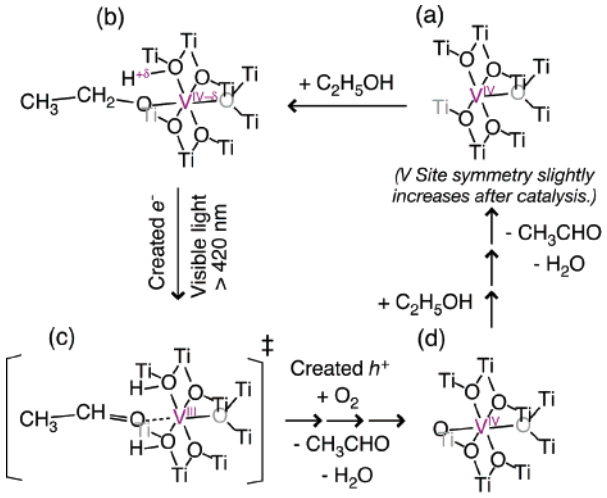

Figure 4. Proposed reaction mechanism of ethanol dehydration over the mesoporous V−TiO_2 catalyst under visible light (a−d).

derived from the spectral difference between the V^{III} site of V_2O_3 and the *unknown, true valence state* V^{III} in mesoporous V−TiO_2.

DISCUSSION

Spectroscopy. The chemical shifts in the V K$\beta_{5,2}$ emission were confirmed to be +3.2 and +1.0 eV between standard V^{III} and V^{IV} and between standard V^{IV} and V^{V} sites, respectively (Table

2 and Figure 1A). The V^{IV}-selective XANES spectrum was successfully obtained by tuning the fluorescence spectrometer to 5459.0 eV among the 1:1 physical mixture of standard V^{IV} and V^{V} compounds (Figure 2B, spectrum a). However, the 1s−3d (mainly) pre-edge peak intensity was enhanced by 2.1 times when compared with the spectrum of $V^{IV}O(SO_4)\cdot nH_2O$ measured in the transmission mode (Figure 2A, spectrum b), probably because of resonance-excitation effects.[18,22] In the XANES tuned to 5464.4 eV, 80% of the V^{V} sites were extracted (Figure 2B, inset of spectrum c) for the 1:1 physical mixture of standard V^{IV} and V^{V} compounds (Figure 2B, spectrum c). Fortunately, in view of the photocatalysis of mesoporous V−TiO_2, the redox cycle was suggested between V^{III} and V^{IV} and the chemical shift in the emission spectra was relatively greater (3.2 eV).

V^{III}-selective XANES was tried for partially reduced mesoporous V−TiO_2, by tuning the fluorescence spectrometer to 5456.3 eV (Figures 1B, spectrum d and 2C, spectrum b). The rising-edge position (5477.4 eV) still corresponded to valence state V^{IV} (Table 2). The spectrum was interpreted to select valence state V^{III} to 60% among the mixture of valence states V^{III} (minor) and V^{IV} (dominant) in the catalyst, based on spectral fits (Figure 2C, inset). The time scale of photocatalysis was reported for electron excitation (≈femtoseconds), electron distribution to V sites (dynamic equilibrium, $\approx 10^2$ ps), and electron donation to the ethoxyl group bound to V (≈milliseconds).[10] The ratio of valence state V^{III} (Figure 4c) should be quite small, in dynamic equilibrium with V^{IV} sites + photoexcited electrons (i.e., short lifetime of valence state V^{III}).

Implications to Catalysis. The V K$\beta_{5,2}$-selecting V K-edge XANES was systematically applied to the mesoporous V−TiO_2 catalyst under several conditions of ethanol-dehydration reaction in visible light. The tuned energy was first fixed to the top of each peak of V K$\beta_{5,2}$ (Figure 1B, arrows) for catalytic comparison. The data was interpreted in combination with V K$\beta_{5,2}$ emission data.

The trend of absorption-edge energy change (Table 2 and Figure 3) was consistent with the V K$\beta_{5,2}$ peak shift (Table 2 and Figure 1B). In both X-ray spectra, the energy corresponding to valence state V^{IV} for the fresh sample progressively shifted toward the V^{III} state in ethanol under visible light. Fully reduced V^{III} was not detected either in V K$\beta_{5,2}$ emission or XANES spectra, but the majority was V^{IV} (emission peak 5461.0−5462.4 eV and absorption edge 5477.8−5479.9 eV, respectively) compared with the corresponding energy ranges (5460.5−5462.3 eV and 5476.9−5479.8 eV, respectively) for standard V^{IV} compounds (Table 2).[12,19−21,28] The shift back to valence state V^{IV} was detected after turning off the visible light, introducing oxygen, and turning visible light on again (Figure 1B-d, e and Figure 3d−f). The reversible energy shifts were reproduced in repeated tests for V K$\beta_{5,2}$ emission and V K-edge absorption measurements.

The 1s−3d (mainly) pre-edge peak remained essentially at the same position, 5468.0−5468.4 eV in Figure 3a−d, but the intensity progressively decreased to 19%. Among the mesoporous V−TiO_2 samples with various loading amounts of V, a systematic increase of the pre-edge peak was observed as the V content increased from 0.6 to 10.4 wt %, because of the decrease of site symmetry, while keeping the rising edge and post-edge features unchanged.[12] Thus, V-site symmetry was lower in the fresh sample (Figure 4a) and became higher because of ethoxyl group adsorption (structure b) and probably because of the remaining oxygen atoms (structure d).

In oxygen under visible light, the pre-edge peak remained at a similar energy (5468.7 eV); however, the intensity gradually grew (Figure 3e,f). The final valence state of vanadium was almost similar to the fresh state, based on XANES (Figure 3a,f) and V K$\beta_{5,2}$ emission (Figure 1B, spectra a, e). However, the intensity of the pre-edge peak did not fully recover but achieved 67% (Figure 3f) of the initial intensity. The site symmetry (coordination number) was lower for the fresh V sites substituting on the Ti sites, associated with a very high specific SA.[17] The symmetry increased after the ethanol dehydration reaction under visible light (Figure 3f).

Water was produced 13 times faster in the first 1 h of the catalysis than in steady state after 1 h (Table 1, entry c).[9] This demonstration of site symmetry increase based on V K$\beta_{5,2}$-selecting XANES is the first report related to photocatalytic time course. The site symmetry change may be more pronounced by selecting the predominant valence state of vanadium in catalyst with the narrow bandwidth of 1.1 eV (Figure 3).

The photocatalytic mechanism is proposed in Figure 4. The redox pair was suggested to be V^{IV} and V^{III}, based on the directions of the V K absorption-edge and V K$\beta_{5,2}$ emission-peak shifts. The impurity-energy level near the conduction band was considered for the V^{IV}-substituting model in TiO_2 (Scheme 1).[10,29] Because the mesoporous TiO_2 phase was amorphous,[12,17,25] the band gap should be greater compared with anatase-type TiO_2 due to quantum-size effects.[1] The reason V doping enhanced the catalysis remarkably only for mesoporous TiO_2 (no/negative effects of V doping on anatase-type TiO_2) in visible light (Table 1, entries b, c)[9] may be the creation of the $V^{IV/III}$ impurity energy level in the relatively greater band gap of mesoporous TiO_2. This energy level is involved in visible light absorption (Scheme 1).

The difference of V valence states may be the primary reason for the different reaction paths of dehydration ($V^{IV} \rightleftarrows V^{III}$) and dehydrogenation (native V^{V})[4,10,12] of ethanol.[9] The V^{IV} sites were effectively exposed to the surface in the mesoporous samples due to the high specific SA (1200−800 $m^2\ g^{-1}$), compared with the V^{IV}−TiO_2 samples prepared via a sol−gel method (10−150 $m^2\ g^{-1}$).[5,6,27,30] In this work, valence state V^{III}, photoreduced from V^{IV}, was observed successfully under the *on-reaction* condition. The availability of V sites should be higher because of the higher dispersion of mesoporous V−TiO_2.

V K$\beta_{5,2}$-selecting XAFS measurements to directly detect valence state V^{III} by increasing the population of V^{III} with a continuous feed of a saturated pressure of ethanol gas, illuminated by visible light, are in progress. When the V K$\beta_{5,2}$ peak shifts within an energy region of V^{III}, theoretical evaluation of the chemical shifts, using FEFF (XES card)[31] for the V site models in Figure 4, will be valuable. When the spectral data for valence states V^{III} and V^{IV} are available for the mesoporous V−TiO_2 catalyst, the population of each valence state can be determined under each catalytic condition.

(29) Nishikawa, T.; Nakajima, T.; Shinohara, Y. *J. Mol. Struct.: THEOCHEM* **2001**, *545*, 67−74.
(30) Balikdjian, J. P.; Davidson, A.; Launay, S.; Eckert, H.; Che, M. *J. Phys. Chem. B* **2000**, *104*, 8931−8939.
(31) Ankudinov, A. L.; Ravel, B.; Rehr, J. J.; Conradson, S. D. *Phys. Rev. B* **1998**, *58*, 7565−7576.

CONCLUSIONS

This paper demonstrated the feasibility of extracting V^{IV} sites from a physical mixture of standard V^{IV} and V^{V} inorganic compounds, by tuning a fluorescence spectrometer to the lower-energy shoulder (5459.0 eV) of the V^{IV} sites. The extraction of V^{V} sites was 80%. Pre-edge peak enhancement was observed in the V^{IV} K$\beta_{5,2}$-selecting XANES tuned to 5459.0 eV.

Partial reduction of native V^{IV} sites in mesoporous V−TiO_2 was observed in V K$\beta_{5,2}$ emission and K$\beta_{5,2}$-selecting V K-edge XANES spectra in ethanol under visible-light. The partially reduced V valence state oxidized back to the initial valence state (V^{IV}) in oxygen and/or under visible light. V-site symmetry (coordination) slightly increased after photocatalysis, based on the decrease of pre-edge peak intensity.

The partially reduced vanadium remained within the energy ranges of valence state V^{IV}. The extraction of photoreduced valence state V^{III} was 60%, by tuning to 5456.3 eV for partially reduced mesoporous V−TiO_2. The small population of valence state V^{III} under dynamic equilibrium with V^{IV} + photoexcited e^- ($\approx 10^2$ ps) was discriminated by V K$\beta_{5,2}$-selecting XAFS, tuned to the lower-energy shoulder.

V doping was effective in creating a $V^{IV/III}$ impurity-energy level for visible-light absorption in the relatively greater band gap of mesoporous TiO_2, because of the quantum-size effect. Catalytic superiority of ultimately exposed (catalytically available) native V^{IV} sites was also suggested.

ACKNOWLEDGMENT

This manuscript is part 22 in the series. X-ray measurements were performed under the approval of the Photon Factory Proposal Committee (Grants 2005P014, 2006G097) and technically supported by Professors M. Nomura and Y. Inada. This work was financially supported from the Grant-in-aid in the priority area "Molecular Nanodynamics" (Y.I. Grant 432-17034013).

SUPPORTING INFORMATION AVAILABLE

Additional information as noted in text. This material is available free of charge via the Internet at http://pubs.acs.org.

Received for review March 2, 2007. Accepted July 11, 2007.

AC070427P